ChemComm

View Article Online
View Journal | View Issue

Check for updates

Large negative linear compressibility of a porous molecular co-crystal†

Szymon Sobczak, [ID] [a] Aleksandra Półrolniczak, [ID] [a] Paulina Ratajczyk, [ID] [a] Weizhao Cai, [ID] [a] Andrzej Gładysiak, [a] Varvara I. Nikolayenko, [ID] [b] Dominic C. Castell, [ID] [b] Leonard J. Barbour [ID] *[b] and Andrzej Katrusiak [ID] *[a]

Flexible and transformable molecules, particularly those responding to external stimuli, are needed for designing sensors and porous compounds capable of storing or separating gases and liquids. Under normal conditions the photochromic compound, 1,2-bis[2-methyl-5-(pyridyl)-3thienyl]cyclopentene (BTCP) forms a porous co-crystal with 1,4-diiodotetrafluorobenzene (dItFB). It traps acetone (Ac) molecules in the pores. Owing to a unique system of pores in the polar framework, the crystal is sensitive to the humidity in the air and to the chosen liquid environment. When compressed in non-penetrating media, the crystal displays a strong negative linear compressibility (NLC) along [100].

The search for environmentally-friendly methods for storing fuels[1–6] and for removing pollution and waste[7–9] drives the current interest in various kinds of porous materials. Crystalline compounds with well-defined pores and cages are especially promising for these purposes. Although the field of porous materials is dominated by microporous zeolites and metal–organic frameworks (MOFs), molecular systems can be attractive for several reasons.[10,11] Owing to the structural and chemical variability generated by modular assembly, it is possible to change the pore sizes and to fine-tune the shape and functionality of the pores in materials free of metal ions. The inclusion of stimulus-responsive molecules can result in unprecedented properties of such porous molecular systems.

Interesting phenomena related to stimulus-responsive compounds include interconversions between isomeric forms and topochemical reactions triggered by light. The molecules of such compounds are conformationally flexible and capable of

undergoing low-energy reactions, involving breaking and forming covalent bonds.

To investigate the high-pressure behaviour of this class of materials we have chosen a bis-3-thienylcyclopentene derivative of 1,2-bis[2′-methyl-5′-(pyrid-4″-yl)-thien-3′-yl]perfluoro-cyclopentene (BTCP).[12–18] When irradiated with ultraviolet light, this group of compounds undergoes solid-state photocyclization, yielding a stable isomeric form with a closed ring. Exposure to visible light results in the ring-open form.[16,18] The reactivity of BTCP, as shown in Fig. 1 derivatives can be triggered in relatively large aggregates. Even single crystals can undergo bulk conversions, involving reversible structural changes, such as pore opening.[16] It is well-known that high pressure often induces prominent changes in crystal structure,[19,20] phase transitions,[21–28] sorption of solvent molecules[29–34] and chemical reactions.[35–41] Moreover, it was found that flexible molecules assembled into aggregates or polymeric frameworks under hydrostatic pressure can exhibit counterintuitive elastic properties, including negative linear and area compression.[36,42–45]

Here we report the isothermal compression of a porous molecular co-crystal solvate, hereafter abbreviated as BTCPs·dItFB·Ac, of 1,2-bis[2′-methyl-5′-(pyrid-4″-yl)-thien-3′-yl]perfluoro-cyclopentene with 1,4-diiodotetrafluorobenzene (dItFB) and acetone (Ac).[46] We have established that in the range of

[a] Department of Chemistry, Adam Mickiewicz University, Poznań, Poland.
E-mail: katran@amu.edu.pl

[b] Department of Chemistry and Polymer Science, University of Stellenbosch,
Matieland 7600, South Africa. E-mail: ljb@sun.ac.za

† Electronic supplementary information (ESI) available: Experimental details, literature survey concerning NLC coefficients, detailed conformational analisis and tabularized detailed crystallographic data. CCDC 1886608–1886615. For ESI and crystallographic data in CIF or other electronic format see DOI: 10.1039/d0cc00461h
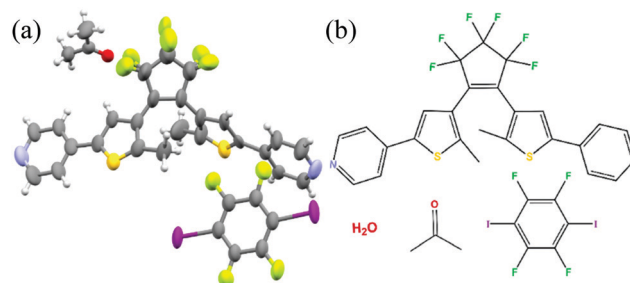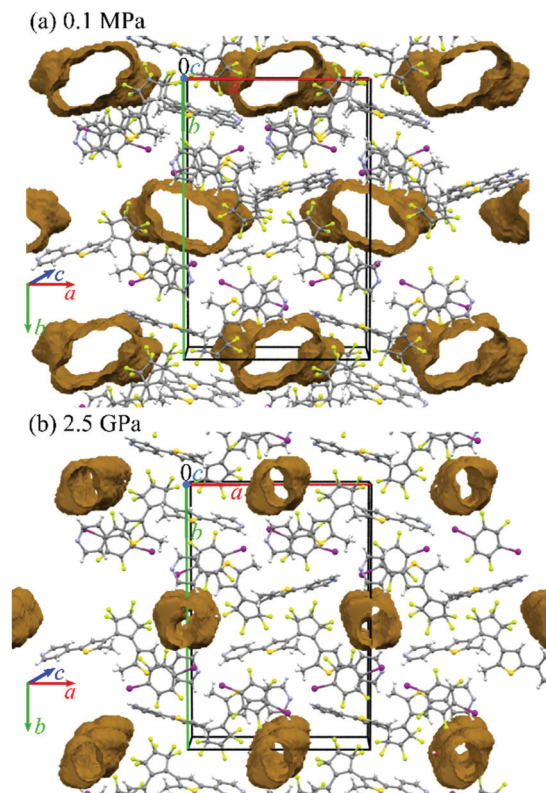

Fig. 1 (a) The asymmetric unit of co-crystal BTCPs·dItFB·Ac and (b) the structural formula of BTCP, dItFB as well as the guests described in our work. In (a), the anisotropic thermal parameters are shown at the 50% probability level and the disordered Ac molecule is shown in one of its half-occupied sites only.

Fig. 2 The size and arrangement of voids (a) at ambient pressure and (b) at 2.5 GPa. The voids are shown for a 1.2 Å probe radius and grid spacing 0.2 Å using the program Mercury.

0–2.5 GPa at room temperature this crystal exhibits pronounced negative linear compressibility (NLC).

BTCP and dltFB co-crystallize from acetone under ambient conditions, with acetone molecules trapped in guest-accessible pockets (Fig. 2). We have established that the crystals lose part of their solvent content when exposed to air, and that the quality of such dried crystals can be recovered with a few drops of water. This results in subsequent improvement of the X-ray diffraction data, yielding higher resolution and a lower R_{int} parameter. The water molecules penetrate the pores of the BTCPs·dItFB·Ac crystal, causing some elongation along [001] (Table 1). The unit cell volume of the partially hydrated co-crystals increases by 10.8(7) Å^3, i.e., 2.7 Å^3 per asymmetric unit. This H_2O adsorption is associated with anisotropic strain

of the crystal: parameters b and c elongate by about 0.07 Å and 0.015 Å, respectively, while parameter a shortens by −0.02 Å (Table 1). However, no water molecules could be located in the crystal structure of the crystals exposed to moisture, which suggests non-stoichiometric sorption of H_2O into disordered positions in the pores. Although the uptake of water in molecular crystals and MOFs usually increases the volume, it has been shown that adsorption of water can also result in a significant reduction of volume.[47–49]

A single crystal of BTCPs·dItFB·Ac, which had been stored in a dry environment, was compressed in glycerol. Although disordered H_2O molecules could not be located up to 1.95 GPa, it was possible to model one water molecule per asymmetric unit at 2.5 GPa. This suggests that their ordering takes place at higher pressure. Karl Fischer titration of the glycerol confirmed the presence of somewhat less that 2% (wt) of water, which could be the origin of the water molecules located in the pores of the compressed sample. Single-crystal X-ray diffraction data were recorded at pressures of 0.4, 0.7, 1.09, 1.59, 1.95 and 2.5 GPa. High-pressure experiments were carried out in a Merrill-Bassett diamond-anvil cell (DAC), modified by mounting the diamond anvils directly on steel supports with conical windows.[50] The DAC was centred using the gasket shadowing method.[51] Starting from the ambient-pressure model, the high-pressure crystal structures were refined using the least-squares method of SHELXL.[52] The pressure in the DAC was calibrated by the ruby fluorescence method, using a Photon Control spectrometer with enhanced resolution, affording an accuracy of 0.02 GPa.[53,54] X-Ray data were measured on a four-circle Oxford-Diffraction Xcalibur diffractometer equipped with an EOS-CCD detector. Due to the strongly disordered acetone molecule in all high-pressure measurements, the SQUEEZE algorithm of PLATON was applied.[55] The crystallographic data and experimental details are summarized in Table 1 and Table S4 (ESI†) and have been deposited in CIF format at the Cambridge Structural Database with numbers CCDC 1886608–1886615.†

Isothermal compression of a single crystal of BTCPs·dItFB·Ac immersed in glycerol induces negative linear compressibility (NLC) along [100], i.e., perpendicular to the pore channels. The NLC of the co-crystal along this direction is unprecedented in magnitude for an organic molecular crystal, reaching −30 TPa^{-1} between 0.1 MPa and 0.4 GPa (cf. Table S1 in the ESI†).[56] The crystal compressibility is clearly nonlinear (Fig. 3) and the NLC magnitude gradually reduces to −15.54 TPa^{-1}

Table 1 Selected crystallographic data of co-crystal BTCP·dItFB·Ac (cf. Table S4 in ESI for details)

Pressure [GPa]	0.0001	0.0001	0.40	0.70	1.09	1.59	1.95	2.50
Environment	Air	Water	Glycerol	Glycerol	Glycerol	Glycerol	Glycerol	Glycerol
Space group	$Pna2_1$	$Pna2_1$	$Pna2_1$	$Pna2_1$	$Pna2_1$	$Pna2_1$	$Pna2_1$	$Pna2_1$
a (Å)	17.2716(8)	17.2451(6)	17.475(9)	17.449(4)	17.559(5)	17.604(14)	17.564(10)	17.606(4)
b (Å)	27.171(3)	27.2415(16)	26.52(5)	26.511(15)	26.315(16)	25.83(6)	25.64(5)	25.580(17)
c (Å)	7.9406(7)	7.9554(3)	7.662(7)	7.536(11)	7.259(8)	7.13(4)	7.07(3)	6.944(9)
V (Å^3)	3726.5(6)	3737.3(3)	3551(8)	3486(5)	3354(4)	3240(20)	3185(15)	3127(5)
Z/Z'	4/1	4/1	4/1	4/1	4/1	4/1	4/1	4/1
D_x (g cm^{-3})*	1.803*	1.808*	1.903*	1.938*	2.014*	2.085*	2.121*	2.161*

*D_x – the initial stoichiometry BTCP·dItFB·Ac without water content was assumed for the density calculations.
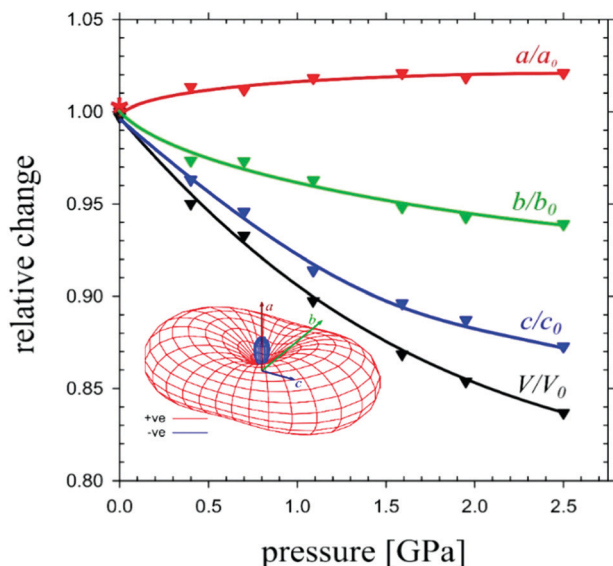
Fig. 3 Compression of co-crystal BTCP·dItFB·Ac in glycerol plotted relative to the 0.1 MPa dimensions. The error bars are smaller than the plotted symbols. The inset shows a graphical representation of the compressibility tensor calculated between the 0.1 MPa and 0.7 GPa (cf. Fig. S3 and Table S3 in ESI†).[56]

between 0.1 MPa and 0.7 GPa, Table S1 (ESI†). The NLC in molecular crystals originates from anisotropic structural features. For the BTCP cocrystal the NLC can be rationalized using the wine-rack mechanism, as the NLC effect occurs along the elongation direction of the cross-section of the pores (compare Fig. 2 and 3). The compression also involves changes in the conformation of molecules, and in their arrangement.

The initial compression up to 0.4 GPa affects the BTCP conformation. The perfluorocyclopentene and heterocyclic aromatic rings of BTCP approximate the shape of an isosceles triangle. The rings are flat and of well-known regular geometry. However, owing to the single bonds that join them, the molecule is flexible. As the pressure increases, the molecule becomes elongated. We have established that the molecular shape of BTCP is most affected by pressure up to 0.4 GPa, when the distance between terminal pyridine rings elongates by 1.7%
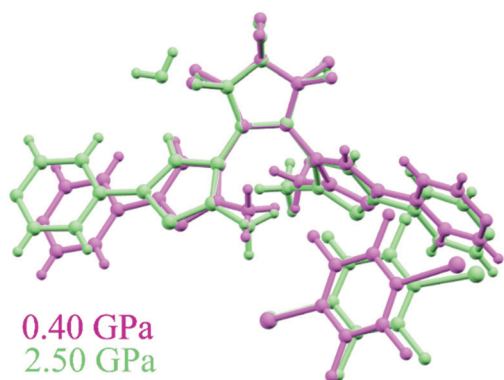

Fig. 4 The two molecules of BTCP from 0.40 GPa and 2.5 GPa superimposed on the perfluorocyclopentene ring.

(compared to 2.4% at 2.50 GPa). This elongation coincides with the NLC effect along [100]. The pressure effect on the intramolecular distance between two reactive carbon atoms in the thienyl groups is unfavourable for closing the ring.[57] Only in the initial pressure range does this distance decrease insignificantly, but at 2.5 GPa it elongates considerably (Fig. 4).

In summary, we have investigated a porous and polar co-crystal solvate BTCP·dItFB·Ac. At ambient conditions, it absorbs or releases water depending on the surrounding moisture. Under pressure, the crystal displays strongly anisotropic compression coupled to the conformation of BTCP molecules. To our knowledge,[43] the negative linear compressibility of over -30 TPa^{-1} is the strongest ever reported for an organic molecular crystal; similarly, we have observed that BTCP·dItFB·Ac displays an impressive positive linear compression of about 90 TPa^{-1}, corresponding to the reduction by 12% at 2.5 GPa of the c unit cell parameter.

Conflicts of interest

There are no conflicts of interest to declare.

Notes and references

1 L. J. Murray, M. Dincă and J. R. Long, *Chem. Soc. Rev.*, 2009, **38**, 1294.
2 J. A. Mason, J. Oktawiec, M. K. Taylor, M. R. Hudson, J. Rodriguez, J. E. Bachman, M. I. Gonzalez, A. Cervellino, A. Guagliardi, C. M. Brown, P. L. Llewellyn, N. Masciocchi and J. R. Long, *Nature*, 2015, **527**, 357–361.
3 W. R. Browne and B. L. Feringa, *Nat. Nanotechnol.*, 2006, **1**, 25–35.
4 A. Dhakshinamoorthy, A. M. Asiri and H. García, *Angew. Chem., Int. Ed.*, 2016, **55**, 5414–5445.
5 M. Gallo and D. Glossman-Mitnik, *J. Phys. Chem. C*, 2009, **113**, 6634–6642.
6 S. Noro, *Metal-Organic Frameworks*, Wiley-VCH Verlag GmbH & Co. KGaA, Weinheim, Germany, 2013, vol. 5.
7 J. Liu, P. K. Thallapally and D. Strachan, *Langmuir*, 2012, **28**, 11584–11589.
8 B. Aguila, D. Banerjee, Z. Nie, Y. Shin, S. Ma and P. K. Thallapally, *Chem. Commun.*, 2016, **52**, 5940–5942.
9 S. Jakobsen, D. Gianolio, D. S. Wragg, M. H. Nilsen, H. Emerich, S. Bordiga, C. Lamberti, U. Olsbye, M. Tilset and K. P. Lillerud, *Phys. Rev. B: Condens. Matter Mater. Phys.*, 2012, **86**, 125429.
10 T. Hasell and A. Cooper, *Nat. Rev. Mater.*, 2016, **1**, 16053.
11 J. R. Holst, A. Trewin and A. I. Cooper, *Nat. Chem.*, 2010, **2**, 915–920.
12 K. Matsuda, Y. Shinkai and M. Irie, *Inorg. Chem.*, 2004, **43**, 3774–3776.
13 F. Luo, C. Bin Fan, M. B. Luo, X. L. Wu, Y. Zhu, S. Z. Pu, W. Y. Xu and G. C. Guo, *Angew. Chem., Int. Ed.*, 2014, **53**, 9298–9301.
14 X. F. Feng, F. Luo, L. Zhang, A. M. Zheng, C. S. Yan, L. Le Gong, C. Bin Fan, H. Q. Wu and Z. Q. Liu, *Chem. Commun.*, 2016, **53**, 763–766.
15 K. Matsuda, K. Takayama and M. Irie, *Chem. Commun.*, 2001, 363–364.

16 H. Sato, R. Matsuda, S. Kitagawa, Y. Zheng, H. J. Jeon and P. Wu, *Nat. Commun.*, 2017, **8**, 100.

17 V. I. Nikolayenko, S. A. Herbert and L. J. Barbour, *Chem. Commun.*, 2017, **53**, 11142–11145.

18 K. Nomiyama, M. Irie, K. Matsuda, M. Isayama, Y. Shinkai and T. Yamaguchi, *Chem. Lett.*, 2003, **32**, 1178–1179.

19 C. Sanloup, *The deep earth*, Springer, Netherlands, Dordrecht, 2012, vol. 140.

20 Elena Boldyreva and P. Dera, *High-Pressure Crystallography*, Springer Science & Business Media, 2010.

21 S. Sobczak and A. Katrusiak, *J. Phys. Chem. C*, 2017, **121**, 2539–2545.

22 E. Patyk, J. Skumiel, M. Podsiadło and A. Katrusiak, *Angew. Chem., Int. Ed.*, 2012, **51**, 2146–2150.

23 M. Fisch, A. Lanza, E. Boldyreva, P. Macchi and N. Casati, *J. Phys. Chem. C*, 2015, **119**, 18611–18617.

24 E. V. Boldyreva, S. N. Ivashevskaya, H. Sowa, H. Ahsbahs and H.-P. Weber, *Dokl. Phys. Chem.*, 2004, **396**, 111–114.

25 Y. Wang, K. Li, A. Sano-Furukawa, F. Hong, H. Zheng, A. Katrusiak, F. Liao, M. Andrzejewski, T. Hattori, L. Wang, H. Mao and Y. Meng, *J. Phys. Chem. C*, 2016, **120**, 29510–29519.

26 F. P. A. Fabbiani, D. R. Allan, A. Dawson, W. I. F. David, P. A. McGregor, I. D. H. Oswald, S. Parsons and C. R. Pulham, *Chem. Commun.*, 2003, 3004–3005.

27 F. P. A. Fabbiani, D. R. Allan, W. I. F. David, A. J. Davidson, A. R. Lennie, S. Parsons, C. R. Pulham and J. E. Warren, *Cryst. Growth Des.*, 2007, **7**, 1115–1124.

28 F. P. A. Fabbiani and C. R. Pulham, *Chem. Soc. Rev.*, 2006, **35**, 932–942.

29 F. X. Coudert, *Chem. Mater.*, 2015, **27**, 1905–1916.

30 S. Sobczak and A. Katrusiak, *Cryst. Growth Des.*, 2018, **18**, 1082–1089.

31 S. C. McKellar and S. A. Moggach, *Acta Crystallogr., Sect. B: Struct. Sci., Cryst. Eng. Mater.*, 2015, **71**, 587–607.

32 S. A. Moggach, T. D. Bennett and A. K. Cheetham, *Angew. Chem., Int. Ed.*, 2009, **48**, 7087–7089.

33 S. A. Moggach, P. A. Wright, S. C. McKellar, A.-M. Banu, A. Greenaway, K. Ward, A. J. Graham, T. Düren and J. P. S. Mowat, *J. Am. Chem. Soc.*, 2014, **136**, 8606–8613.

34 J. Liu, S. Li, K. Yang, B. Zou, G. Zou, K. Wang, B. Liu and Q. Li, *J. Phys. Chem. C*, 2014, **118**, 5848–5853.

35 M. Andrzejewski and A. Katrusiak, *J. Phys. Chem. Lett.*, 2017, **8**, 929–935.

36 W. Cai, A. Gładysiak, M. Anioła, V. J. Smith, L. J. Barbour and A. Katrusiak, *J. Am. Chem. Soc.*, 2015, **137**, 9296–9301.

37 J. P. Tidey, H. L. S. Wong, J. McMaster, M. Schröder and A. J. Blake, *Acta Crystallogr., Sect. B: Struct. Sci., Cryst. Eng. Mater.*, 2016, **72**, 357–371.

38 J. E. Warren, M. Murrie, S. A. Moggach, P. Parois, A. R. Lennie, N. Rowantree, S. Parsons, E. K. Brechin and K. W. Galloway, *CrystEngComm*, 2009, **11**, 2601.

39 R. J. Angel, N. L. Ross, E. C. Spencer, J. A. K. Howard and B. E. Hanson, *J. Am. Chem. Soc.*, 2009, **131**, 4022–4026.

40 J. K. Clegg, A. J. Brock, K. A. Jolliffe, L. F. Lindoy, S. Parsons, P. A. Tasker and F. J. White, *Chem. – Eur. J.*, 2017, **23**, 12480–12483.

41 A. Półrolniczak, S. Sobczak and A. Katrusiak, *Inorg. Chem.*, 2018, **57**, 8942–8950.

42 W. Li, M. R. Probert, M. Kosa, T. D. Bennett, A. Thirumurugan, R. P. Burwood, M. Parinello, J. A. K. Howard and A. K. Cheetham, *J. Am. Chem. Soc.*, 2012, **134**, 11940–11943.

43 A. B. Cairns and A. L. Goodwin, *Phys. Chem. Chem. Phys.*, 2015, **17**, 20449–20465.

44 R. H. Baughman, S. Stafström, C. Cui and S. O. Dantas, *Science*, 1998, **279**, 1522–1524.

45 W. Zieliński and A. Katrusiak, *Cryst. Growth Des.*, 2014, **14**, 4247–4253.

46 V. I. Nikolayenko, D. C. Castell, D. P. van Heerden and L. J. Barbour, *Angew. Chem., Int. Ed.*, 2018, **57**, 12086–12091.

47 W. Zieliński and A. Katrusiak, *CrystEngComm*, 2015, **17**, 5468–5473.

48 M. Andrzejewski, N. Casati and A. Katrusiak, *Dalton Trans.*, 2017, **46**, 14795–14803.

49 V. I. Nikolayenko, A. Heyns and L. J. Barbour, *Chem. Commun.*, 2017, **53**, 11306–11309.

50 L. Merrill and W. A. Bassett, *Rev. Sci. Instrum.*, 1974, **45**, 290–294.

51 A. Budzianowski and A. Katrusiak, High-pressure crystallographic experiments with a CCD detector, in *High-Pressure Crystallography*, ed. A. Katrusiak and P. F. McMillan, Kluwer Academic Publisher, Dordrecht.

52 G. M. Sheldrick, *Acta Crystallogr., Sect. C: Struct, Chem.*, 2015, **71**, 3–8.

53 G. J. Piermarini, S. Block, J. D. Barnett and R. A. Forman, *J. Appl. Phys.*, 1975, **46**, 2774–2780.

54 H. K. Mao, J. Xu and P. M. Bell, *J. Geophys. Res.*, 1986, **91**, 4673–4676.

55 A. L. Spek, *Acta Crystallogr., Sect. C: Struct, Chem.*, 2015, **71**, 9–18.

56 M. J. Cliffe and A. L. Goodwin, *J. Appl. Crystallogr.*, 2012, **45**, 1321–1329.

57 X. Lin, J. Jia, P. Hubberstey, M. Schröder and N. R. Champness, *CrystEngComm*, 2007, **9**, 438–448.